 http://dx.doi.org/10.14500/aro.12195

Evaluation of 3D-CRT Treatment Planning Techniques for Breast Cancer: A Comparative Study of Collapsed Cone and Monte Carlo Algorithms Using New Quality Indices

Riyadh S. Agid[1,2†] and Fatiheea F. Hassan[1]

[1]Department of Basic Sciences, College of Medicine, Hawler Medical University
Erbil, Kurdistan Region – F.R. Iraq

[2]Department of Physics, College of Science, Salahaddin University,
Erbil, Kurdistan Region – F.R. Iraq

***Abstract*—This study compares the collapsed cone (CC) and Monte Carlo (MC) algorithms for radiation treatment planning for lumpectomy of the chest wall. The aim is to evaluate how these algorithms affect dose distribution and plan quality improve treatment outcomes. Fifteen patients received left breast chest wall radiation using the 3D-conformal radiotherapy (3D-CRT) technique with CC calculation. Then plans were subsequently recalculated using the MC algorithm on the same treatment planning system. Dosimetric parameters assessed included the planning target volume (PTV), homogeneity index (HI), and conformity index. In this research, new plan quality indicators named index of achievement, index of hotness, and index of coldness were also evaluated. Organs at risks (OARs) analyzed included the ipsilateral lung, contralateral breast, heart, and spinal cord, and their data were retrieved from the dose-volume histogram (DVH) and compared among algorithms. The results indicated that both algorithms effectively covered PTV. The MC algorithm improved HI and reduced the DVH high dose to the prescribed dose. Interestingly, the CC algorithm resulted in lower mean dose to OAR, particularly the heart and ipsilateral lung, suggesting better OAR sparing. The new quality indexes, the MC algorithm demonstrated superior "index of achievement" values, indicating improved dose painting and better dose conformity within the target. In addition, the MC showed a sharper dose fall-off outside the PTV, thereby improving target coverage and overall plan quality. In conclusion, the MC algorithm provides enhanced dose homogeneity and better target coverage quality, while the CC algorithm offers improved OAR protection.**

***Index Terms*–3D-CRT techniques, Collapsed cone and Monte Carlo algorithms, Dose-volume histogram, Planning target volume, Quality plan indices.**

ARO-The Scientific Journal of Koya University
Vol. XIII, No.2 (2025), Article ID: ARO.12195. 8 pages
DOI: 10.14500/aro.12195
Received: 13 April 2025; Accepted: 27 July 2025
Regular research paper; Published: 22 August 2025
†Corresponding author's e-mail: riyadh.agid@su.edu.krd

I. Introduction

Breast cancer is the most commonly diagnosed cancer among women worldwide (Fuentes, et al., 2024). Radiation therapy (RT) is a common and effective treatment for breast cancer. Ionizing radiation targets and aimed at destroying or inhibiting the growth of malignant tumor cells, helping prevent local and regional recurrence (Abdulkareem and Hassan, 2020). One of the primary challenges of RT is delivering an effective dose to the tumor region, particularly the chest wall and nearby lymph nodes, while minimizing radiation exposure to healthy surrounding tissues. Among the common techniques used are 3D-conformal radiotherapy (3D-CRT), volumetric-modulated arc therapy, and intensity-modulated radiotherapy, each designed to improve tumor coverage and spare organs at risks (OARs) (Alsaihaty, et al., 2024) (Saddik, 2023). Technological Advancements, such as multi-leaf collimators, have further enhanced the precision and efficiency of 3D-CRT (Rastogi, et al., 2018). However, the accurate dose distribution relies on the precision of the treatment planning system (TPS) algorithms. The collapsed cone (CC) algorithm uses a ray-tracing method for fast but less accurate results in heterogeneous regions (Zaghian, et al., 2021). The Monte Carlo (MC) method, while more time-consuming, provides higher accuracy by simulating individual particle interactions, especially in heterogeneous tissues.

Several studies have focused on improving dose distribution using homogeneity index (HI) and conformity index (CI) to evaluate TPS (Petrova, Smickovska and Lazarevska et al., 2017), (Liu, et al., 2016). However, in this study, a novel evaluation approach is the 1st time by applying a new quality index based on dose painting (DP) analysis from dose-volume histogram (DVH). This new index provides a more detailed and spatially sensitive assessment of plan quality, allowing for a more precise evaluation of dose distribution within the target and OAR. For instance, Park et al., (2014), introduced the "index of achievement"

(IOA) to overcome the limitations of traditional DP software. This indicator considers the biological impact of the dose. However, due to uncertainties associated with IOA, its correlation with biological effects is not guaranteed (Park, et al., 2014) (Palma, et al., 2010). In addition, indexes such as IOA, index of hotness (IOH), and index of coldness (IOC) are underexplored in terms of their practical application in clinical decision making.

The present study aims to compare 3D-CRT plans for left lumpectomy breast cancer using CC and MC dose calculation algorithms by analyzing planning target volume (PTV) dosimetry, evaluating new quality indices (IOA, IOH, and IOC), and OAR dose based on DVHs.

II. Materials And Methods

A. Patient Selection

This study includes 15 female breast cancer patients, all of whom had left breast tumors. Each patient underwent a lumpectomy, a surgical procedure that removes the breast cancer tumor while preserving the surrounding breast tissue. The patients were initially planned using 3D-CRT with CC dose estimations. For this study, the MC algorithm was employed to recalculate the same treatment plans on the same TPS.

Patients were positioned supine on breast boards with arms raised and the head turned away from the treated breast Fig. 1. The computed tomography (CT) images were acquired using a 16-slice CT scanner (5 mm slice thickness) from the superior neck to the inferior diaphragm (Prabhakar, et al., 2009), at the Awat Radiation Oncology Center in Erbil. A radiation oncologist contoured the PTV and OAR, including the heart, lungs, spinal cord, and both breasts.

B. Treatment Planning

Mono-isocentric plans were retroactively developed using the Monaco (Elekta Solutions AB, Stockholm, Sweden) TPS software, version 6.1.4.0. A total dose of 4005 cGy in 15 fractions over 3 weeks (267 cGy per session) was prescribed dose, following UK radiotherapy dose fractionation guidelines (Murshed, 2024). The PTV size ranged from 329.485 cm^3 to 1487.32 cm^3, with a median value of 1217.645 cm^3.

The planning objective was to deliver 95% of the prescribed dose of PTV while minimizing exposure to OAR. Hot spots (doses exceeding 108% of the prescribed dose) were allowed only within the PTV. OARs in this study were based on the quantitative analysis of normal tissue effects in the Clinic (QUANTEC) 2010 guidelines (Bentzen, et al., 2010).

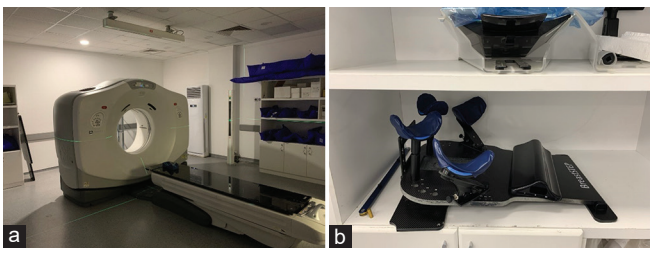

Fig. 1. Computed tomography (CT) unit at Awat Radiation Oncology Center, Erbil (a) CT simulation (b) Breast board.

C. Plan Evaluation

DVHs were generated for each plan after the designed beam was computed using the dose calculation algorithm in the TPS. The cumulative DVH for each treatment plan was used to derive the dosimetric parameters for the PTV and OARs.

The dosimetric parameters for the PTV included the percentage of the PTV volume receiving a dose ≥95% of the prescribed dose (V95) and the percentage of the PTV volume receiving a dose ≥107% of the prescribed dose (V107). The PTV was evaluated for D98% (the minimum dose received by at least 98% of the PTV), D2% (the maximum dose received by at least 2% of the PTV), and D50% (the median dose received by 50% of the PTV). The maximum, mean, and minimum doses for the PTV, as well as the total monitor units (MU), were also recorded. The treatment objectives were to achieve V95 ≥ 95% of the PTV volume and V107 < 10 cc (centimeter cubic) of the PTV volume.

The OARs evaluated in this study included the normal ipsilateral and contralateral lung, heart, spinal cord, and esophagus. The dosimetric parameters for the normal lung included the mean dose (Dmean) and volumes of the ipsilateral lung receiving specific doses V_x (V5, V10, V18, V30). For the heart, in addition to Dmean, the volume of the heart receiving specific doses (max, min, mean, V22.5, and V10) was recorded. The maximum dose (Dmax) for the spinal cord and the mean dose to the esophagus were also documented. The recommended dose constraints for the OARs are shown in Table I.

After generating 3D-CRT plans in MONACO, DVHs were exported as comma separated values files for dose comparison. These cumulative cDVH files were converted into differential dDVHs by TPS software (Pyakuryal et al., 2010). The CSV format ensuring cross system compatibility and can be easily analyzed using spreadsheet tools such as Excel. Park et al. introduce the IOA to assess dose homogeneity in dose DP.

D. HI and CI

The HI and CI were calculated based on "International Commission on Radiation Units and Measurements" (ICRU

TABLE I
Recommended Dose Limits for Normal Tissue Tolerance (Bisello, et al., 2022)

Volume	Dose volume parameter	Endpoints
Ipsilateral Lung	V5 <50% V10 <40% V18 <35% V30 <15% Dmean ≤20 Gy	Symptomatic pneumonitis (Marks, et al., 2010)
Heart	Dmean <26 Gy V25 <10%	Pericarditis Long-term cardiac mortality
Contralateral breast	V3 <%10	
Spinal cord	Dmax <40Gy	Myelopathy

Report 83) and the RT Oncology Group, respectively (Menzel, 2012) to evaluate dose uniformity and conformity.

$$HI = \frac{D2\% - D98\%}{D50\%} \quad (1)$$

Where D98% is the minimum dose received by at least 98% of the PTV, D2% is the maximum dose received by at least 2% of the PTV, and D50% is the median dose received by 50% of the PTV. Ideal HI values are close to zero, with higher values indicating less homogeneous dose distribution.

CI formula is expressed as:

$$\mathrm{CI} = \frac{\mathrm{PIV}}{\mathrm{TV}} \quad (2)$$

TV is the total target volume, and PIV is the prescription isodose volume (95% of the prescribed dose). A CI of 1 indicates optimal coverage; CI > 1 suggest overdose to the target and healthy tissue, while values <1 indicate under coverage of the TV.

E. The Plan Quality Index Formulas

In 2014, (Park, et al., 2014). introduced the IOA, which assesses how closely the planned dose distribution aligns with the required dosage in a dose DP radiotherapy plan (Park, et al., 2014). The IOA values were calculated using established plan quality index methods as follows:

$$\mathrm{IOA} = 1 + \sqrt{\sum_i \left[\left(\frac{D_{i,Plan} - D_{i,Rx}}{D_{i,Rx}} \right)^2 X \frac{v_i}{V} \right]} \quad (3)$$

Other indicators, such as IOH and IOC, reflect the extent of overdose or underdose in the target. DVH is used to evaluate IOH and IOC, by identifying areas of overdose (hot spots) or underdose within the TV.

$$\mathrm{IOH} = 1 + \sqrt{\sum_i \left[\left(\frac{D_{i,Plan} - D_{i,Rx}}{D_{i,Rx}} \right)^2 X \frac{v_i}{V} \right]} \quad (v_i = 0 \ if \ D_{i,plan} \le D_{i,Rx}) \quad (4)$$

$$\mathrm{IOC} = 1 - \sqrt{\sum_i \left[\left(\frac{D_{i,Plan} - D_{i,Rx}}{D_{i,Rx}} \right)^2 X \frac{v_i}{V} \right]} \quad (v_i = 0 \ if \ D_{i,plan} \ge D_{i,Rx}) \quad (5)$$

V is the target's total volume of target, vi, Di is the ith bin of the differential dDVH (derived from DVH CSV files generated by the commercial TPS Monaco), which is the volume of the ith voxel in the TV and "Di, Rx and Di, Plan" are the ith voxel's prescribed and planned doses respectively.

F. Statistical Analysis

Test for normal distribution was performed using a "Shapiro–Wilk" test in the Statistical Package for the Social Sciences 27.0 for statistical analysis.

For normally distributed data, statistical significance was tested using Student *t*-test was used for comparison. For a distribution showing small deviation from a normal distribution, a "Mann–Whitney" test was utilized. Statistical significance was compared against a threshold p = 0.05.

III. Results

A. Dosimetric Parameters of the PTV and MU

The PTV for all treatment plans (3D-CRT technique calculated using the MC and CC algorithms) was evaluated. A total of 15 3D-CRT plans were developed to compare the dosimetric parameters between the two algorithms. Table II summarizes the PTV results in terms of V95, Dmax, Dmin, Dmean, D98%, D50%, D2%, HI, CI, and MU. There was no significant difference between the CC and MC algorithms in terms of PTV coverage (V95) (95.78 vs. 95.532, p = 0.619), as shown in Fig. 2. Most plans achieved PTV target coverage of V95 ≥ 95%, except for three plans (Plan 8 for CC and Plans 2 and 3 for MC). Similar results were observed for D50% (4116.7 vs. 4113.61, p = 0.260) cGy. The MC algorithm was noted to be better at reducing the tail of the DVH. The mean dose (Dmean) ranged from 4080.52 cGy for CC to 4077.626 cGy for MC (p = 0.340), showing that the mean dose received by the PTV was slightly higher than the prescribed dose.

Regarding the volume of the PTV receiving doses >107% of the prescribed dose (V107), the results show that most plans had V107 < 10 cm^3 of the PTV, except for one plan with V107 > 10 cc, which occurred with the CC algorithm. The V107 values ranged from 0.1 cc to 10.379 cc for CC and from 1.06 cc to 9.614 cc for MC. This indicates that there were no significant hotspots in the PTV volume, and the objective of V107 < 10 cc was met in the majority of the plans.

The values for Dmin, Dmax for the PTV, as well as MU for the accelerator head collimator are outlined in Table II. The Dmin to the PTV ranges from 554.7 cGy to 3019.8 cGy for CC and from 524.1 cGy to 2910.9 cGy for MC. For Dmax to the PTV, the values range from 4316.6 cGy to 4371.4 cGy for CC and from 4330.5 cGy

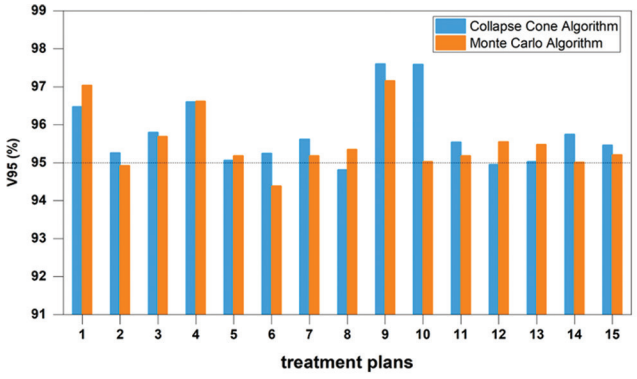

Fig. 2. Distribution of the V95 of the planning target volume for all studied treatment plans. The objective is V95 ≥ 95% shown as the dashed line on the graph.

TABLE II
DOSIMETRIC PARAMETERS OF THE PTV AND OAR FOR LEFT SIDE OF BREAST CASES USING CC AND MC ALGORITHM

Target and OAR	Collapse Cone Algorithm (3D-CRT)			Monte Carlo Algorithm (3D-CRT)			p-value
	Range	Median	Average	Range	Median	Average	
PTV							
V95 ≥95%	94.81–97.6	95.54	95.786±0.8938	94.38–97.16	95.21	95.532±0.796	0.619
V107 <10cc	0.1–10.379	4.636	5.208±3.641	1.06–9.614	6.389	5.912±2.9602	0.313
D2% cGy	4234.7–4278.4	4268.1	4261.68±13.99	4243.9–4277.6	4263.5	4261.42±9.574	0.052
D98% cGy	3482.1–3779.9	3697	3670.14±83.8	3550.7–3775.8	3674.5	3675.5±65.678	0.313
D50% cGy	4069.8–4162	4113	4116.7±28.4	4077.2–4149.9	4117.4	4113.61±21.844	0.260
Dmin cGy	554.7–3019.8	1461.9	1698.92	524.1–2910.9	1399.3	1595.08	0.655
Dmax cGy	4316.6–4371.4	4337.8	4336.2	4330.5–4647.9	4364.7	4387.633	0.075
Dmean cGy	4053.1–4123.7	4074.3	4080.52	4050.8–4115.8	4074.2	4077.626	0.340
CI	0.9480–0.9765	0.95536	0.9579±0.0090	0.9437–0.97164	0.952	0.9553±0.00807	0.608
HI	0.11425–0.19112	0.13842	0.14362±0.0212	0.11912–0.17370	0.14230	0.14240±0.0160	0.238
MU	279.91–333.91	318.58	316.9	292.11–341.23	316.05	316.73	0.817
Ipsilateral Lung							
Dmean <2000cGy	576.5–1287.4	855.7	878.07	610.9–1358.5	895.9	921.986	0.233
V5 <50%	21.63–48.5	32.21	33.968±7.11	22.57–72	34.13	37.59±11.96	0.267
V10 <40%	15.27–38.49	23.94	25.11±6.23	15.45–39.38	23.96	25.334±6.407	0.806
V18 ≤35%	11.75–31.6	18.85	19.8±5.36	11.95–32.17	19.01	20.046±5.477	0.870
V30 <15%	7.63–23.18	13.06	13.54±4.15	8.274–24.8	13.76	14.378±4.350	0.325
Contralateral lung							
V18 ≤35%	0.00	0.00	0.00	0.00	0.00	0.00	
Contralateral breast							
Dmean <100 cGy	62.9–95.7	74.6	76.1±10.04	55.31–53.5	74.1	81.513±24.464	0.076
V3 <10%	0–1.92	0.11	0.3973±0.6196	0–5.120	0.11	0.626±1.3089	1.00
Heart							
V22.5 ≤10%	0–6.62	2.9	3.357±2.14	0.01–6.93	3.01	3.29±2.0011	0.563
Dmean <300–500 cGy	138.4–460.8	322.4	314.9	155.4–489.6	361.9	340.14	0.861
Spinal cord							
Dmax <4000cGy	2658.2–3762.9	3196.45	3209.39	2733.9–3817.7	3292.65	3314.9	0.596

PTV: Planning target volume, OAR: Organ at risk, CI: Conformity index, HI: Homogeneity index, cc: Volume, Dmax: Max dose; Dmean: Mean dose, D2: D50, D98: Dose received by 2%, 50%, 98% of volume; V3, V5, V10, V18, V22.5, V30, V95, volume received by 3%, 5%, 18%, 22.5%, 30%, 95% prescribed dose

to 4647.9 cGy for MC. The MU to the accelerator head collimator has an average value of 316.9 for CC and 316.73 for MC.

B. Dosimetric Parameters to OARs

This research compared the dosage constraints for OAR with the guidelines outlined in the QUANTEC (Bentzen et al., 2010), (Marks et al., 2010). Table II summarizes the dosimetric parameters for OAR evaluated using both algorithms. The doses received by normal tissues, including the ipsilateral and contralateral lungs, heart, spinal cord, and contralateral breast, were assessed and reviewed by a qualified radiation oncologist.

C. Ipsilateral and Contralateral Lung

As shown in Fig. 3, for the ipsilateral lung (i.e., the lung on the same side as the treatment), all plans had a mean dose (Dmean) of <2000 cGy, and V18 values were below 35%. The mean dose in the ipsilateral lung ranged from 576.5 to 1287.4 cGy for the CC algorithm and from 610.9 to 1358.5 cGy for the MC algorithm. For the contralateral lung (i.e., the lung on the opposite side of the treatment), V18 was zero for all plans, as shown in Table II. All plans demonstrated that the Dmean and V18 values for both the ipsilateral and contralateral lungs were relatively low and below the dose constraints recommended by QUANTEC (Dmean <2000 cGy and V18 <35%).

For the ipsilateral lung, the V5, V10, V18, and V30 values were lower in CC plans compared to MC plans. Specifically, these values were:

CC: V5 = 33.968%, V10 = 25.11%, V18 = 19.8%, V30 = 13.54%.

MC: V5 = 37.59%, V10 = 25.334%, V18 = 20.046%, V30 = 14.378%.

These results are depicted in Fig. 4 (Bisello et al., 2022).

D. Heart

A mean heart dose of <500 cGy was required as the dose constraint for the heart. The mean heart dose achieved by the CC algorithm was 314.9 cGy, while the MC algorithm resulted in a mean dose of 340.14 cGy ($p = 0.861$). This difference was not statistically significant, indicating that both algorithms were equally effective in controlling the heart dose for left-sided breast cancer patients.

Similarly, the required dose constraint for the percentage of heart volume receiving 22.5 Gy (V22.5) should be kept below 10%, as shown in Fig. 5. When evaluating the mean percentage of heart volume receiving 22.5 Gy, the MC algorithm allowed for a lower mean percentage (V22.5 = 3.29%) compared to the CC algorithm (V22.5 = 3.357%) ($p = 0.563$).

http://dx.doi.org/10.14500/aro.12195

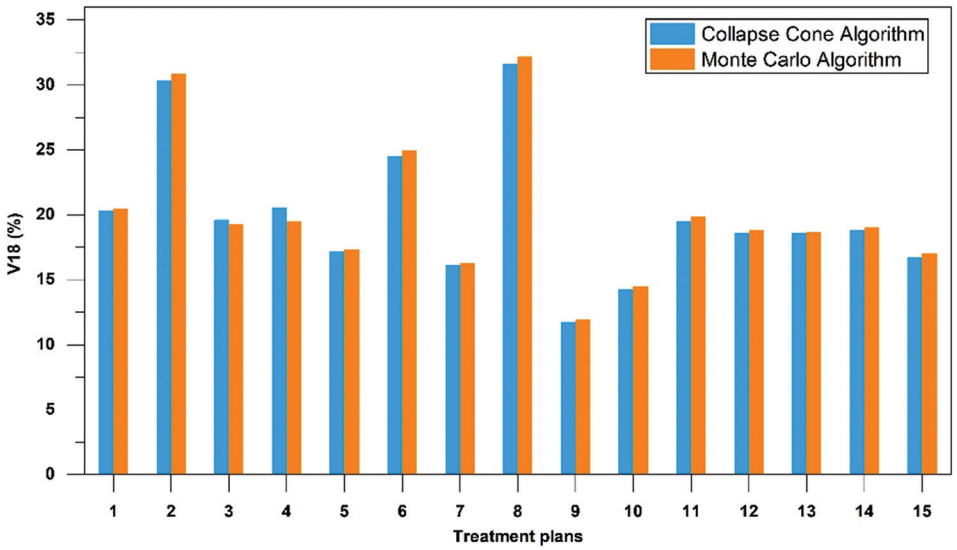

Fig. 3. The distribution of the V18 parameter to the left lung cases. The dose constraint is V18 <35%.

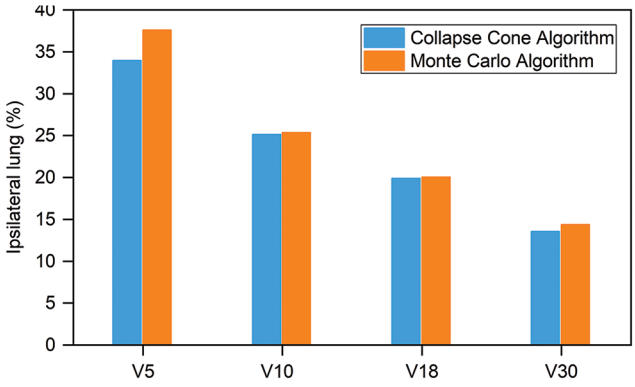

Fig. 4. Compares the dosimetric parameters of mean ipsilateral lung tissue with both calculation algorithm. At low doses of V5, V10, V18, and V30, the dose of the ipsilateral lung.

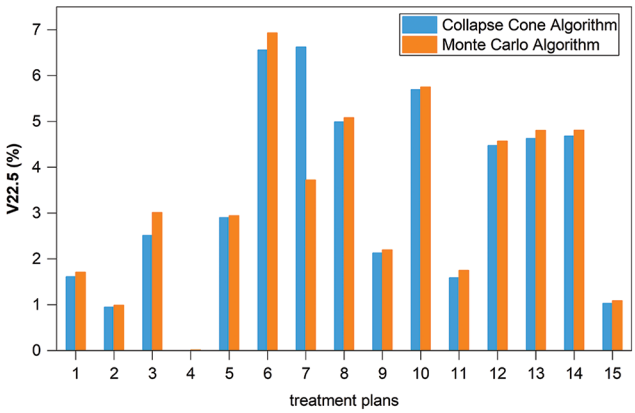

Fig. 5. The distribution of the V22.5 parameter to the heart. The dose constraint is V22.5 ≤ 10%.

E. Spinal Cord

The maximum spinal cord dose achieved by the CC algorithm was 3209.39 cGy, compared to 3314.9 cGy for the MC algorithm (p = 0.596), as shown in Fig. 6. This result again favors the CC algorithm over the MC algorithm. The required dose constraint for the maximum spinal cord dose is <4000 cGy.

Using the CC method, the contralateral breast received an average dose of 76.1 cGy, while the MC approach delivered an average dose of 81.513 cGy. The difference between these values was statistically insignificant (p = 0.076).

F. Conformity and HI

The mean values of the CI and HI for both algorithms are shown in Figs. 7 and 8. The mean CI values for both algorithms are outlined in Table II.

The plan using the CC algorithm demonstrated less conformity in dose distribution compared to the MC algorithm. The CI values were 0.9579 ± 0.0090 for CC and 0.9553 ± 0.00807 for MC plans. The difference was not statistically significant (p = 0.608).

The HI indicated that the dose distribution in the MC plans was more homogeneous, with a mean value of 0.14240 ± 0.0160, compared to the CC plans, which had a mean value of 0.14362 ± 0.0212. This difference was not statistically significant (p = 0.238), as shown in Table II.

G. Feasibility of IOA, IOH, and IOC

Due to the constancy and reproducibility of the DVH plot, IOH, and IOC values for breast 3D-CRT are determined and shown in Fig. 9. Fig. 9 shows a value of 1 indicates an exact correspondence between the prescribed and plan dose; values deviating from 1 indicate increased discrepancy. IOC has values equal to or <1, indicating underdosing of the TV, whereas the IOH has values equal to or higher than.

Table III summarizes the computed outcomes of the new indexes. All indicators were classified into three categories (achievement, hotness, and coldness) for further individual analysis. Individual plan evaluations were established for each index using the computed values of the indices. The mean values for IOA, IOH, and IOC with both planning algorithms

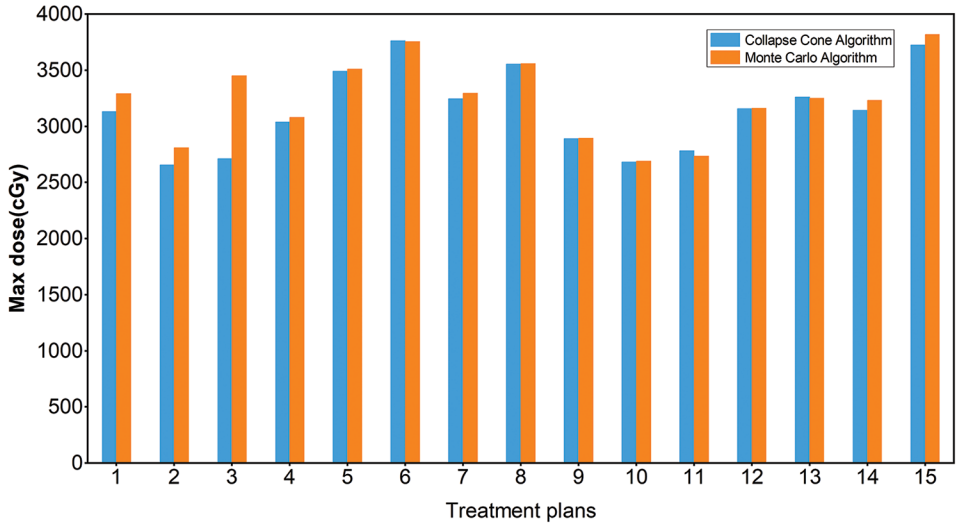

Fig. 6. Distribution of the maximum dose (Dmax) received by the spinal cord in 15 treatment plans for left-sided breast cancer. Contralateral Breast.

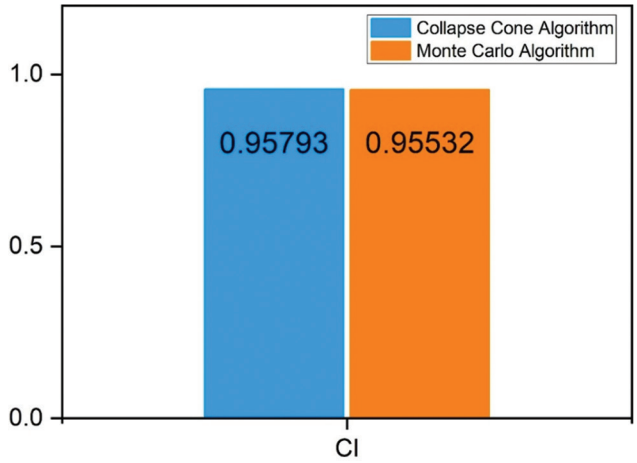

Fig. 7. Comparison of the conformity index between the collapsed cone and Monte Carlo algorithms.

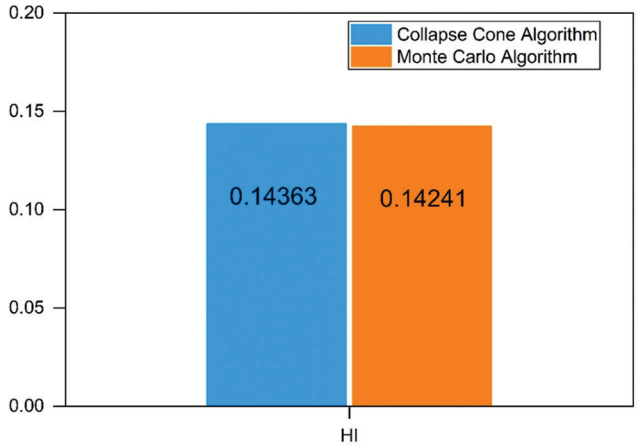

Fig. 8. Comparison of the homogeneity index between the collapsed cone and Monte Carlo algorithms.

were 1.043473792, 1.034466694, and 0.974178852 for CC, 1.04195834, 1.033405227, and 0.975337924 for MC. According to the results, one may notice that no significant

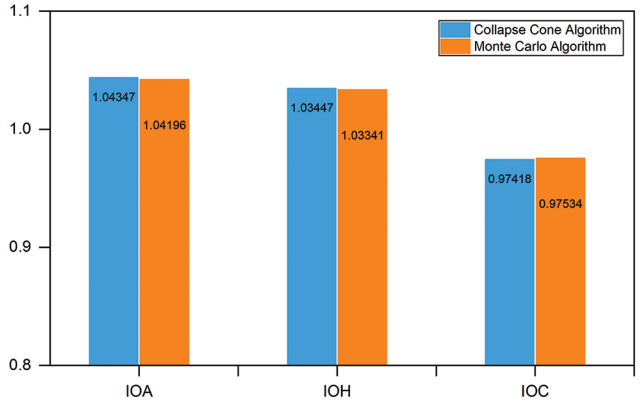

Fig. 9. Achievement, hotness, and coldness from 3D-CRT treatment plans using both the collapsed cone and Monte Carlo algorithms.

TABLE III
CALCULATION RESULTS OF THE IOA, IOH, AND IOC FOR TWO ALGORITHM CASES PLANNED WITH CC AND MC ALGORITHMS

Indices	Collapse Cone Algorithm (3D-CRT)	Monte Carlo Algorithm (3D-CRT)	p-value
	Mean±SD	Mean±SD	
IOA	1.043473792±0.007153	1.04195834±0.004932153	0.129
IOH	1.034466694±0.004506112	1.033405227±0.003456744	0.152
IOC	0.974178852±0.008298226	0.975337924±0.007188929	0.564

IOA: Index of achievement, IOH: Index of hotness, IOC: Index of coldness, SD: Standard deviation

difference was observed. IOA, IOH, and IOC as a result, the dose distribution in the DP region is better for MC as compared CC.

IV. DISCUSSION

This study evaluated CC and MC algorithms in the Monaco 3D-CRT breast cancer planning system.

The CC and MC algorithms provided similar PTV coverage (V95), with both algorithms reaching the clinical goal of 95% PTV coverage. The CC approach approximates photon scatter

and attenuation for more even dose coverage. In comparison, MC models do deposition more accurately. It provides exact dose distributions in heterogeneous media such as lung or bone, where scatter and attenuation effects are crucial (Kim, Kim and Kim 2015). Tissue heterogeneity and complicated scattering effects may cause small localization. Breast cancer tissue densities are usually homogeneous. In such cases, CC reduced photon interaction modeling produces consistent and therapeutically acceptable dose distributions. Due to the breast anatomy's low tissue heterogeneity, CC is adequate for accurate dose estimations.

These findings align with recent research comparing dose metrics in tangent breast plans generated using CC and MC algorithms. Goss, et al., 2023 found that both methods covered PTVs identically with similar V95 values (Goss, et al., 2023). The D50% values were 4116.7 cGy for the CC algorithm and 4113.61 cGy for the MC algorithm, with a $p = 0.260$. The MC algorithm demonstrated better reduction of the DVH tail, which is significant because the tail typically represents lower-dose areas affecting non-target tissues or OAR. By improving particle interaction and scatter modeling, the MC algorithm produces sharper dose fall-off, thereby reducing tissue dosage in these areas (Bhushan et al., 2021). For both algorithms, the mean dose (Dmean) was slightly higher than the allowed dose, likely as an intentional strategy to ensure complete PTV coverage. Clinically acceptable minor overdosage is sometimes used to prevent underdosing important tumor regions (Shaverdian, et al., 2016).

The CC and MC algorithms required an average of 316.9 and 316.73 MU, respectively, for radiation treatment planning. These values reflect both operational efficiency and dosimetric accuracy. A reduction in MU is associated with fewer scattering lines from the accelerator head collimator, which may help reduce the risk of cancer recurrence (Huang et al., 2013).

The mean dose distribution in the ipsilateral lung ranged from 576.5 to 1287.4 cGy for CC and 610.9 to 1358.5 cGy for MC. The slightly broader dose distribution range observed with the MC algorithm can be attributed to its more comprehensive modeling of treatment beams and the physical and geometric characteristics of patient anatomy. This study also found that the CC algorithm's dose predictions closely align with those of the MC algorithm.

The CC plans showed lower V5, V10, V18, and V30 values for the ipsilateral lung compared to the MC plans, although these differences were not statistically significant. To optimize lung dose distribution, the study recommends using advanced dose calculation algorithms such as MC. These findings are consistent with the work of Zhao et al., (2014).

The mean heart dose was 314.9 cGy for the CC algorithm and 340.14 cGy for the MC algorithm ($p = 0.861$), with the volume receiving 22.5 Gy (V22.5Gy) being slightly lower in the CC algorithm by 3.29% compared to the MC algorithm, which showed a 3.357% difference ($p = 0.563$). Rancati, et al., (2007) highlighted that the most critical factor influencing cardiac mortality is the increase in the 22.5 Gy volume, which should be kept below 10% in the long term for the entire heart (Aras, İkizceli and Aktan 2019).

The CC method achieved a CI of 0.9579 ± 0.0090, while the MC algorithm yielded a CI of 0.9553 ± 0.00807. Although the difference was not statistically significant ($p = 0.608$), CC plans were marginally more conformal. Regarding the HI, MC plans had a mean HI of 0.14240 ± 0.0160, while CC plans had a mean HI of 0.14362 ± 0.0212, indicating a slightly more homogeneous dose distribution with the MC approach. However, this difference was also not statistically significant ($p = 0.238$). Our findings are consistent with those of (Zhao, et al., 2014), who reported similar CI and HI values for both the CC and MC algorithms.

In conformal radiation treatment planning, analysis tools such as the homogeneity and CI are commonly used. However, there is no standardized method for calculating, as it has many different definitions and calculation approaches (Carrie, et al., 1995), (Shaw, et al., 1993). To overcome this, three novel plan quality indices were introduced based on Park, et al., (2014). The IOA measured prescription target achievement, whereas the IOH and IOC measured hot and cold regions.

IOA, IOH, and IOC averaged 1.043473792, 1.034466694, and 0.974178852 for CC and 1.04195834, 1.033405227, and 0.975337924 for MC (both planning methods). Despite that, these findings show no substantial difference between the algorithms. While the dosage distribution in the DP area is somewhat better with MC than CC. These findings match (Dashnamoorthy, et al., 2022), (Skórska, et al., 2016) observations.

Our research found that the DVH, supported by IOA, IOH, and IOC indices, can evaluate treatment quality plans and detect overdose and less than prescribed dose. This research is important since it is the first to measure IOA, IOH, and IOC in hot and cold indices using DVH data for breast cancer TPS. This work presents the IOH, and IOC, unlike other studies mostly analyzing dose conformity indices and suggests that DVH alone cannot detect hot and cold spot regions as supplementary measures of radiation dose distribution. Lee, Cao and Kim found that the DVH is useful for analyzing dose-volume coverage but not for dose distribution features such as hot, cold spots, and homogeneity (Lee, Cao and Kim, 2015).

V. Conclusion

In this present work, the CC and MC algorithms were compared, showing that IOH and IOC provide more accurate assessments of overdose and underdose relative to the prescribed dose. Dose homogeneity was improved by the MC algorithm, while the CC algorithm exhibited better conformity in dose distribution. The new quality index, IOA, also shows that the dose distribution in the DP area is better with MC than with CC. Our results further indicate that the MC algorithm provides enhanced dose homogeneity and better target coverage quality, while the CC algorithm offers improved OAR protection.

Ethical Approval

This study was approved by the Research Ethics Committee of the College of Medicine (No. 46, September 22, 2024) Hawler Medical University, Erbil, Kurdistan Region, Iraq.

References

Abdulkareem, N.K., and Hassan, F.F., 2020. Half beam technique in patient with left breast cancer and evaluate its dosimetry parameters from dose-volume histograms. *Medico Legal Update*, 20(2), p.281.

Alsaihaty, Z., Manan, H.A., Sabarudin, A., and Yahya, N., 2024. Hybrid treatment planning for chest wall irradiation utilizing three-dimensional conformal radiotherapy (3DCRT), intensity-modulated radiation therapy (imrt), and volumetric modulated arc therapy (VMAT): A systematic review. *Cureus,* 16(5), p.e59583.

Aras, S., İkizceli, T., and Aktan, M., 2019. Dosimetric comparison of three-dimensional conformal radiotherapy (3D-CRT) and intensity modulated radiotherapy techniques (IMRT) with radiotherapy dose simulations for left-sided mastectomy patients. *European Journal of Breast Health*, 15(2), pp.85-89.

Bentzen, S.M., Constine, L.S., Deasy, J.O., Eisbruch, A., Jackson, A., Marks, L.B., Ten Haken, R.K., and Yorke, E.D., 2010. Quantitative analyses of normal tissue effects in the clinic (QUANTEC): An introduction to the scientific issues. *International Journal of Radiation Oncology Biology Physics*, 76(3), pp.S3-S9.

Bhushan, M., Tripathi, D., Yadav, G., Kumar, L., Chowdhary, R.L., Pahuja, A.K., Suresh, T., Shukla, S.K., and Mitra, S., 2021. Feasibility of monte-carlo algorithm in comparison with collapse-cone dose calculation algorithm of a commercial treatment planning system in the presence of high-density metallic implant: A dosimetric study. *Journal of the Egyptian National Cancer Institute,* 33, p.2.

Bisello, S., Cilla, S., Benini, A., Cardano, R., Nguyen, N.P., Deodato, F., Macchia, G., Buwenge, M., Cammelli, S., Wondemagegnehu, T., Uddin, A.F.M.K., Rizzo, S., Bazzocchi, A., Strigari, L., and Morganti, A.G., 2022. Dose-volume constraints for organs at risk in radiotherapy (CORSAIR): An "all-in-one" multicenter-multidisciplinary practical summary. *Current Oncology*, 29(10), pp.7021-7050.

Carrie, C., Ginestet, C., Bey, P., Aletti, P., Haie-Meder, C., Briot, E., Resbeut, M., Coste, G., Chauvel, P., and Brassard, N., 1995. Conformal radiation therapy. Federation nationale des centres de lutte contre le cancer (FNCLCC). *Bulletin du Cancer,* 82(5), pp.325-330.

Dashnamoorthy, S., Rajamanickam, K., Jeyasingh, E., Pandey, V.P., Nachimuthu, K., Ahmed, I., and Venkatraman, P., 2022. Comparison of dose statistics of intensity-modulated radiation therapy plan from varian eclipse treatment planning system with novel python-based indigenously developed software. *Progress in Medical Physics*, 33(3), pp.25-35.

Fuentes, J.D.B., Morgan, E., De Luna Aguilar, A., Mafra, A., Shah, R., Giusti, F., Vignat, J., Znaor, A., Musetti, C., Yip, C.H., Van Eycken, L., Jedy-Agba, E., Piñeros, M., and Soerjomataram, I., 2024. Global stage distribution of breast cancer at diagnosis: A systematic review and meta-analysis. *JAMA Oncology*, 10(1), pp.71-78.

Goss, M., Champ, C., Trombetta, M., Shamsesfandabadi, P., Demartino, V., Wegner, R., Beriwal, S., and Eisen, V., 2023. The comparison of collapsed cone and monte carlo algorithms in tangential breast planning. *Journal of Radiotherapy in Practice*, 22, p.e94.

Huang, J.Y., Followill, D.S., Wang, X.A., and Kry, S.F., 2013. Accuracy and sources of error of out-of field dose calculations by a commercial treatment planning system for intensity-modulated radiation therapy treatments. *Journal of Applied Clinical Medical Physics*, 14(2), p.4139.

Kim, S.J., Kim, S.K., and Kim, D.H., 2015. Comparison of pencil-beam, collapsed-cone and monte-carlo algorithms in radiotherapy treatment planning for 6-MV photons. *Journal of the Korean Physical Society*, 67, pp.153-158.

Lee, S., Cao, Y.J., and Kim, C.Y., 2015. Physical and radiobiological evaluation of radiotherapy treatment plan. In: *Evolution of Ionizing Radiation Research.* IntechOpen, London.

Liu, H., Chen, X., He, Z., and Li, J., 2016. Evaluation of 3D-CRT, IMRT and VMAT radiotherapy plans for left breast cancer based on clinical dosimetric study. *Computerized Medical Imaging and Graphics*, 54, pp.1-5.

Marks, L.B., Yorke, E.D., Jackson, A., Ten Haken, R.K., Constine, L.S., Eisbruch, A., Bentzen, S.M., Nam, J., and Deasy, J.O., 2010. Use of normal tissue complication probability models in the clinic. *International Journal of Radiation Oncology Biology Physics*, 76(3), pp.S10-S19.

Menzel, H.G., 2012. The international commission on radiation units and measurements. *Journal of the ICRU*, 12(2), pp.1-2.

Murshed, H., 2024. *Fundamentals of Radiation Oncology: Physical, Biological, and Clinical Aspects*. Elsevier, Netherlands.

Palma, D.A., Verbakel, W.F., Otto, K., and Senan, S., 2010. New developments in arc radiation therapy: A review. *Cancer Treatment Reviews*, 36(5), pp.393-399.

Park, Y.K., Park, S., Wu, H.G., and Kim, S., 2014. A new plan quality index for dose painting radiotherapy. *Journal of Applied Clinical Medical Physics*, 15(4), p.4941.

Petrova, D., Smickovska, S., and Lazarevska, E., 2017. Conformity index and homogeneity index of the postoperative whole breast radiotherapy. *Open Access Macedonian Journal of Medical Sciences*, 5(6), pp.736-739.

Prabhakar, R., Ganesh, T., Rath, G.K., Julka, P.K., Sridhar, P.S., Joshi, R.C., and Thulkar, S., 2009. Impact of different CT slice thickness on clinical target volume for 3D-conformal radiotherapy. *Medical Dosimetry*, 34(1), pp.36-41.

Pyakuryal, A., Myint, W.K., Gopalakrishnan, M., Jang, S., Logemann, J.A. & Mittal, B.B.J.J.O.a.C.M.P., 2010. A computational tool for the efficient analysis of dose-volume histograms for radiation therapy treatment plans. *Journal of Applied Clinical Medical Physics*, 11(1), pp.137-157.

Rancati, T., Wennberg, B., Lind, P., Svane, G., and Gagliardi, G., 2007. Early clinical and radiological breast cancer radiation pulmonary complications following therapy: NTCP fit with four different models. *Radiotherapy and Oncology,* 82(3), pp.308-316.

Rastogi, K., Sharma, S., Gupta, S., Agarwal, N., Bhaskar, S., and Jain, S., 2018. Dosimetric comparison of IMRT versus 3DCRT for post-mastectomy chest wall irradiation. *Radiation Oncology Journal*, 36(1), pp.71-78.

Saddik, M.Z., and Hassan, F.F., 2023. Intensity Modulated Radiation and Volumetric Modulated Arc Therapies in Breast Cancer. *Journal of Medicinal and Chemical Sciences*, 6, pp.1925-1934.

Shaverdian, N., Tenn, S., Veruttipong, D., Wang, J., Hegde, J., Lee, C., Cao, M., Agazaryan, N., Steinberg, M., Kupelian, P., and Lee, P., 2016. The significance of PTV dose coverage on cancer control outcomes in early stage non-small cell lung cancer patients treated with highly ablative stereotactic body radiation therapy. *The British Journal of Radiology*, 89(1059), p.20150963.

Shaw, E., Kline, R., Gillin, M., Souhami, L., Hirschfeld, A., Dinapoli, R., and Martin, L., 1993. Radiation therapy oncology group: Radiosurgery quality assurance guidelines. *International Journal of Radiation Oncology Biology Physics*, 27(5), pp.1231-1239.

Skórska, M., Piotrowski, T., Ryczkowski, A., and Kaźmierska, J., 2016. Comparison of treatment planning parameters for dose painting head and neck plans delivered with tomotherapy. *The British Journal of Radiology*, 89(1060), p.20150970.

Zaghian, R., Pashaki, A.S., Haghparast, A., Gholami, M.H., and Mohammadi, M., 2021. Investigation of collapsed-cone algorithm accuracy in small fields and heterogeneous environments. *Journal of Biomedical Physics and Engineering,* 11(2), pp.143-150.

Zhao, Y., Qi, G., Yin, G., Wang, X., Wang, P., Li, J., Xiao, M., Li, J., Kang, S., and Liao, X., 2014. A clinical study of lung cancer dose calculation accuracy with Monte Carlo simulation. *Radiation Oncology*, 9, p.287.